Electronic Supplementary Information

Photochemical synthesis and device application of acene-phenacene hybrid molecules, dibenzo[n]phenacenes (n = 5–7)

Yanting Zhang,[a] Ritsuko Eguchi,*[a] Shino Hamao,[a] Kenta Goto,[b] Fumito Tani,[b] Minoru Yamaji,[c] Yoshihiro Kubozono[a] and Hideki Okamoto*[d]

[a] Research Institute for Interdisciplinary Science, Okayama University, Okayama 700-8530, Japan.

[b] Institute for Materials Chemistry and Engineering, Kyushu University, Fukuoka 819-0395, Japan.

[c] Division of Molecular Science, Graduate School of Science and Engineering, Gunma University, Ota 373-0057, Japan.

[d] Division of Earth, Life, and Molecular Sciences, Graduate School of Natural Science and Technology, Okayama University, Okayama 700-8530, Japan.

Contents

Experimental

1. Synthesis of materials 3
2. NMR, MS, and elemental analyses 7

NMR spectra of novel compounds 8

3. X-ray diffraction (XRD) measurements and atomic force microscopy (AFM) …. 13
4. UV-Vis absorption and photoelectron yield measurements 13
5. Synthesis of **DBnP** single crystals 13
6. Device fabrication of single-crystal FETs 14
7. Device fabrication of thin film FETs 15

Results

1. X-ray diffraction patters 16
2. UV-Vis absorption and photoelectron yield spectra 17
3. Surface morphology of **DBnP** thin films 18
4. Optical microscope images of **DBnP** single crystals 18
5. Typical FET performances of **DBnP** single crystal FETs 19
6. Typical FET performances of **DBnP** thin film FETs 21

Tables 23

Additional References 27

Experimental

1. Synthesis of materials

1-1. (*E*)-1,2-Bis(1-anthryl)ethene 2

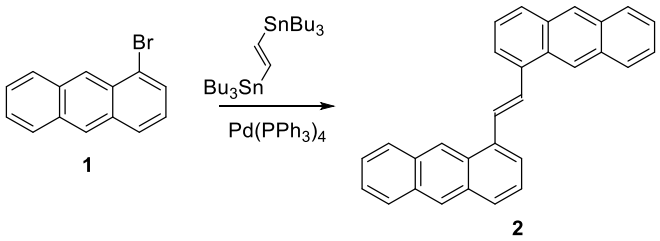

A solution of 1-bromoanthracene **1** (257 mmol), (*E*)-1,2-bis(tributylstannyl)ethene (274 mg, 0.45 mmol), and $Pd(PPh_3)_4$ (52 mg, 0.045 mmol) in toluene (30 ml) was refluxed under an N_2 atmosphere for 13 h. The resulting solution was filtered through a short silica-gel column containing 5% K_2CO_3. After removal of the solvent, the residue was washed with toluene/hexane (1/1 mixt.) to afford (*E*)-1,2-bis(1-anthryl)ethene **2** (148 mg, 86%).

Yellow crystals, mp 286–288°C (Lit 277–279°C)[1]

^{1}H NMR (600 MHz, $CDCl_3$) δ_H 8.84 (s, 2H), 8.50 (s, 2H), 8.15 (s, 2H), 8.08–8.00 (m, 6H), 7.93 (d, 2H, J = 6.7 Hz), 7.58 (dd, 2H, J = 8.4, 6.3 Hz), 7.52–7.45 (m, 4H).

^{13}C NMR (151 MHz, $CDCl_3$) δ_C 135.59, 131.96, 131.80, 131.58, 130.03, 129.31, 128.66, 128.58, 127.93, 126.97, 125.68, 125.61, 125.23, 123.48, 122.76.

Anal. Calcd for $C_{30}H_{20}$, C, 94.70; H, 5.30. Found, C, 94.70; H, 5.36.

1-2. Dibenzo[*b*,*n*]picene (DP5P)

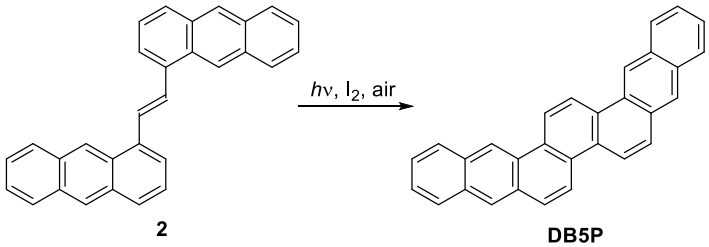

A solution of bis(anthryl)ethene **2** (200 mg, 0.53 mmol) and a small portion of I_2 in toluene (200 ml) was irradiated with black-light lamps (352 nm, 6×16 W) for 8.5 h. the precipitate formed was collected and recrystallized from *o*-dichlorobenzene (**A**, 37 mg). The filtrate was

further irradiated for 14 h and the filtrate was collected and recrystallized from *o*-dichlorobenzene (**B**, 11 mg). The filtrate was concentrated and the obtained yellow solid (79 mg) was dissolved in toluene (200 ml) and a small portion of I_2 was added. The resulting solution was irradiated with the black-light lamps with heating at 85–100°C for 20 h. The precipitate formed was collected and recrystallized from *o*-dichlorobenzene (**C**, 32 mg). The total amount of the obtained **DB5P** (**A** + **B** + **C**) was 81 mg (40%).

Pale yellow fine plates, mp >300°C.

^{1}H NMR (600 MHz, 1,1,2,2-tetrachloroethane-d_2, 80°C) δ_H 9.39 (s, 2H), 9.20 (s, 2H), 9.69 (d, 2H, *J*= 9.2 Hz), 8.54 (s, 2H), 8.26 (d, 2H, *J* = 7.5 Hz), 8.14 (two doublets overlap, 4H), 7.76–7.60 (m, 4H).

^{13}C NMR was not observed due to the low solubility.

Anal. Calcd. for $C_{30}H_{18}$: C, 95.21; H, 4.79. Found: C, 94.51; H, 4.72.

1-3. 4-Ethenylbenzo[*a*]anthracene 4

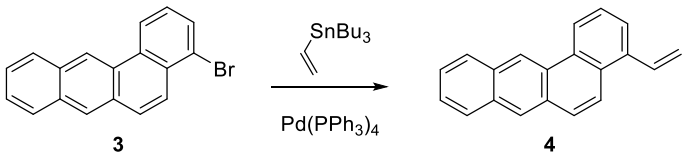

3 4

A mixture of 4-bromobenzanthracene[2] (600 mg, 1.96 mmol), tributylvinyltin (746 mg, 2.35 mmol), and $Pd(PPh_3)_4$ (113 mg, 0.10 mmol) in toluene (30 ml) was refluxed for 15 h. The insoluble materials formed was filtered off and the filtrate was passed through a short silica-gel column containing K_2CO_3 (10wt%) to afford 4-vinylbenzo[*a*]anthracene **4** (404 mg, 81%). Recrystallization from toluene produced off-white plates of product **4**.

Off-white plates, mp. 191–192°C.

^{1}H NMR (600 MHz, $CDCl_3$) 9.18 (s, 1H), 8.81 (d, 1H, *J* = 8.0 Hz), 8.37 (s, 1H), 8.13 (m, 1H), 8.05 (m, 1H), 7.97 (d, 1H, *J* = 9.3 Hz), 7.83 (d, 1H, *J* = 7.8 Hz), 7.76 (d, 1H, *J* = 7.0 Hz), 7.66 (t, 1H, *J* = 7.8 Hz), 7.59–7.51 (m, 3H), 5.82 (dd, 1H, *J* = 17.2, 1.1 Hz), 5.54 (dd, 1H, *J* = 10.8, 1.1 Hz).

^{13}C NMR (151 MHz, $CDCl_3$) 136.48, 134.93, 132.14, 132.10, 130.80, 130.37, 129.36, 129.12, 128.63, 127.85, 127.62, 126.83, 126.70, 126.01, 125.88, 125.38, 122.86, 122.72, 122.04, 117.73.

HRMS (FAB) *m*/*z* calcd. for $C_{20}H_{14}$, 254.1096 [M^+]. Found, 254.1100.

1-4. (*E*)-1-(1-Anthryl)-2-(4-benzo[*a*]anthryl)ethene 5

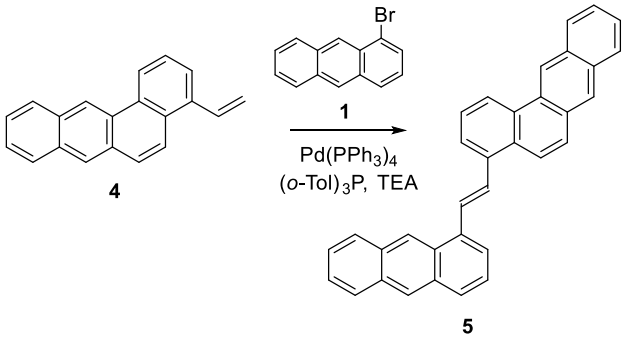

A mixture of vinylbenzoanthracene **4** (300 mg, 1.18 mmol), 1-bromoanthacene **1** (306 mg, 1.19 mmol), (*o*-Tol)$_3$P, and Pd(OAc)$_2$ in DMF (5 ml) and TEA (3 ml) was evacuated and backfilled with Ar three times. The resulting mixture was heated at 80°C for 17 h. After being cooled to r.t., The precipitate formed was collected and washed with a 1 : 1 mixture of toluene and EtOH to afford (*E*)-1-(1-anthryl)-2-(4-benzo[*a*]anthryl)ethene **5** (334 mg, 65%) as greenish-yellow fine needles. mp >300°C

^{1}H NMR (600 MHz, 1,1,2,2-tetrachloroethane-d_2, 90°C) δ_H 9.24 (s, 1H), 8.90 (d, 1H, J = 8.0 Hz), 8.28 (s, 1H), 8.49 (s, 1H), 8.40 (s, 1H), 8.20–8.12 (m, 2H), 8.10–7.99 (m, 7H), 7.91–7.7.83 (m, 2H), 7.79 (t, 1H, J = 7.6 Hz), 7.61–7.52 (m, 3H), 7.51–7.44 (m, 2H).

^{13}C NMR (151 MHz, 1,1,2,2-tetrachloroethane-d_2, 90°C) δ_C 136.31, 135.61, 132.26, 132.22, 132.15, 131.98, 131.76, 131.14, 130.43, 130.17, 129.99, 129.89, 129.65, 129.19, 128.66, 128.62, 128.55, 127.94, 127.78, 127.73, 127.01, 126.82 (2C), 126.06, 125.93, 125.79, 125.71 (2C), 125.31, 123.60, 122.96, 122.86, 122.83, 122.05.

Anal. Calcd. for $C_{34}H_{22}$; C, 94.85; H, 5.15. Found; C, 94.85%; H, 5.13%.

1-5. Benzo[*b*]naphtho[2, 3-*m*]picene (DB6P)

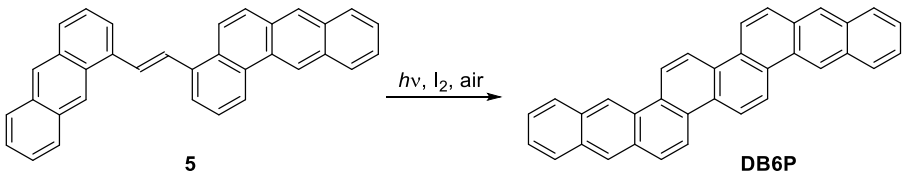

A solution of (*E*)-1-(1-anthryl)-2-(4-benzo[*a*]anthryl)ethane **5** (200 mg, 0.46 mmol) and a small portion of I_2 in *o*-dichlororbenzene (300 mol) was heated at 85–100°C and irradiated with black-light lamps (352 nm, 6×16 W) for 7.2 h. The precipitate formed was collected (63 mg, **A**). The filtrate was irradiated with the black-light lamps for 12.5 h and the precipitated product was collected (26 mg, **B**). The total yield of the product (**A** + **B**) was 89 mg (45%).

Pale yellow plates, mp >300°C.

1H NMR (600 MHz, 1,1,2,2-tetrachloroethane-d_2, 80°C) δ_H 9.14 (s, 2H), 9.19 (d, 2H, J = 8.8 Hz), 9.09 (d, 2H, J = 9.0 Hz), 8.83 (d, 2H, J = 8.7 Hz), 8.58 (s, 2H), 8.27 (brd, 2H, J = 7.4 Hz), 8.22 (d, 2H, J = 8.7 Hz), 8.15 (brd, 2H, J = 7.1 Hz), 7.64 (m, 4H).

^{13}C NMR spectra were not observed due to the low solubility of **DB6P**.

Anal. calcd. for $C_{34}H_{20}$; C, 95.30; H, 4.70. Found; C, 94.54; H, 4.46.

1-7. (*E*)-1,2-Bis(4-benzoanthryl)ethene 6

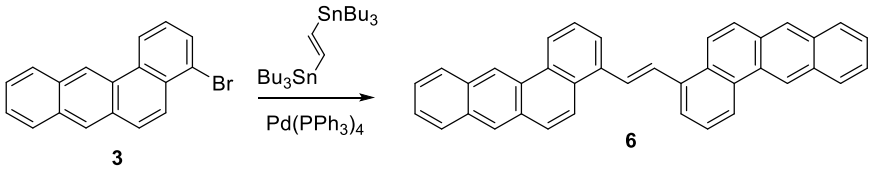

A mixture of 4-bromobenzo[*a*]anthracene **3** (612 mg, 2.0 mmol), trans-1,2-bis(tributylstannyl)ethene (547 mg, 0.9 mmol), and $Pd(PPh_3)_4$ (231 mg, 0.20 mmol) was refluxed under an Ar atmosphere for 24 h. The precipitate formed was collected and washed with toluene to afford (*E*)-1,2-bis(4-benzo[*a*]anthryl)ethene **6** 358 mg (37%). Recrystallization from *o*-dichlorobenzene gave pale brown plates.

Pale brown plates, mp >300°C.

^{1}H NMR (600 MHz, 1,1,2,2-tetrachloroethane-d_2, 80°C) δ_H 9.25 (s, 2H), 8.91 (d, 2H, J = 8.3 Hz), 8.34 (s, 2H), 8.21–8.14 (m, 4H), 8.12–8.07 (m, 2H), 8.054 (d, 2H, J = 7.1 Hz), 8.00 (s, 2H), 7.92 (d, 2H, J = 9.3 Hz), 7.81 (t, 2H,J = 7.6 Hz), 7.65–7.57 (m, 4H).

^{13}C NMR spectrum was not observed due to low solubility.

Anal. Calcd. for $C_{38}H_{24}$, C, 94.97; H, 5.03. Found, C, 94.63; H, 4.85.

1-8. Benz[*b*]anthra[2,1-*m*]picene (DP7P)

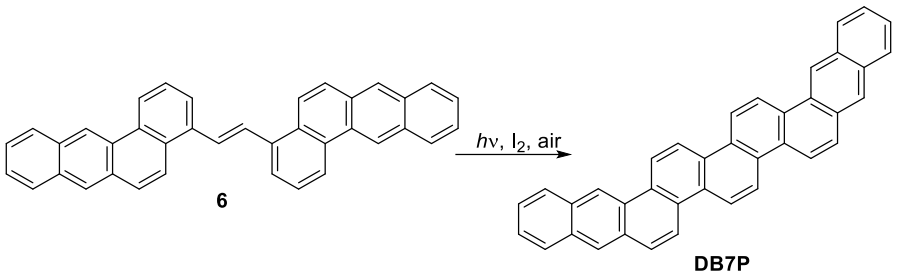

A solution of (*E*)-1,2-bis(4-benzo[*a*]anthryl)ethene **6** (150 mg, 0.31 mmol) and a small portion of I_2 in *o*-dichlorobenzene (300 ml) was heated at *ca*. 125°C and the solution was irradiated with black-light lamps (365 nm, 6×16W) at the temperature for 2.2 h. The precipitate formed was collected and washed with boiling *o*-dichlorobenzene to afford **DB7P** (129 mg, 86%).

Pale yellow plates, mp >300°C.

^{1}H and ^{13}C NMR spectra were not observed due to the low solubility od **DB7P**.

Anal. Calcd. for $C_{38}H_{22}$, C, 95.37; H, 4.63. Found, C, 95.26; H, 4.39.

2. NMR, MS and elemental analyses

^{1}H and ^{13}C NMR spectra were recorded on VARIAN NMR System 600 (600 MHz) and JEOL ECZ600 (600 MHz) spectrometers. Elemental analyses were measured on a PERKIN-ELMER 2400II CHN-S analyser at the Micro Elemental Analysis Laboratory of Okayama University. High-resolution mass spectra (FAB) were recorded on a JEOL JMS-700 MStation spectrometer at Institute for Materials Chemistry and Engineering, Kyushu University.

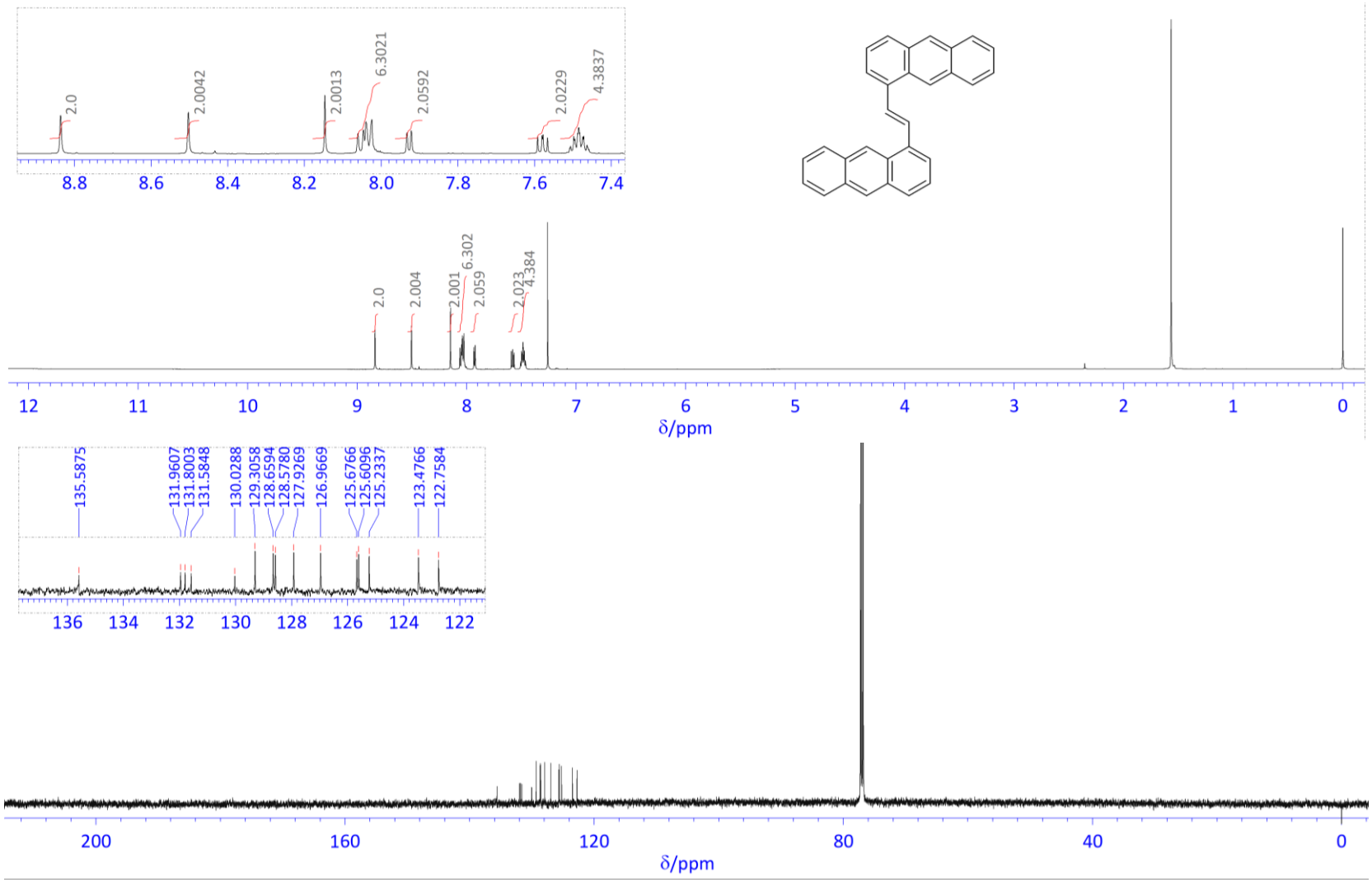

Figure S1. ^{1}H (600 MHz) and ^{13}C (151 MHz) NMR spectra of compound **2** ($CDCl_3$).

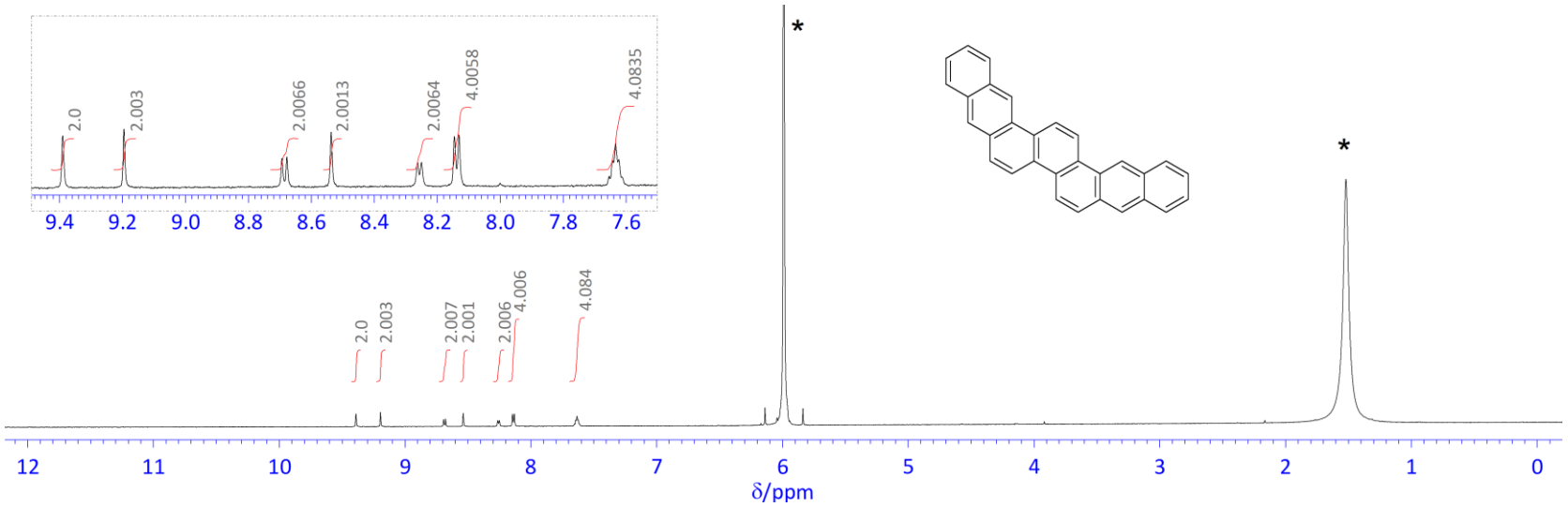

Figure S2. ^{1}H NMR spectrum of **DB5P** (600 MHz, 1,1,2,2-tetrachloroenthane-d_2, at 80°C). Asterisked signals are due to the solvent and water.

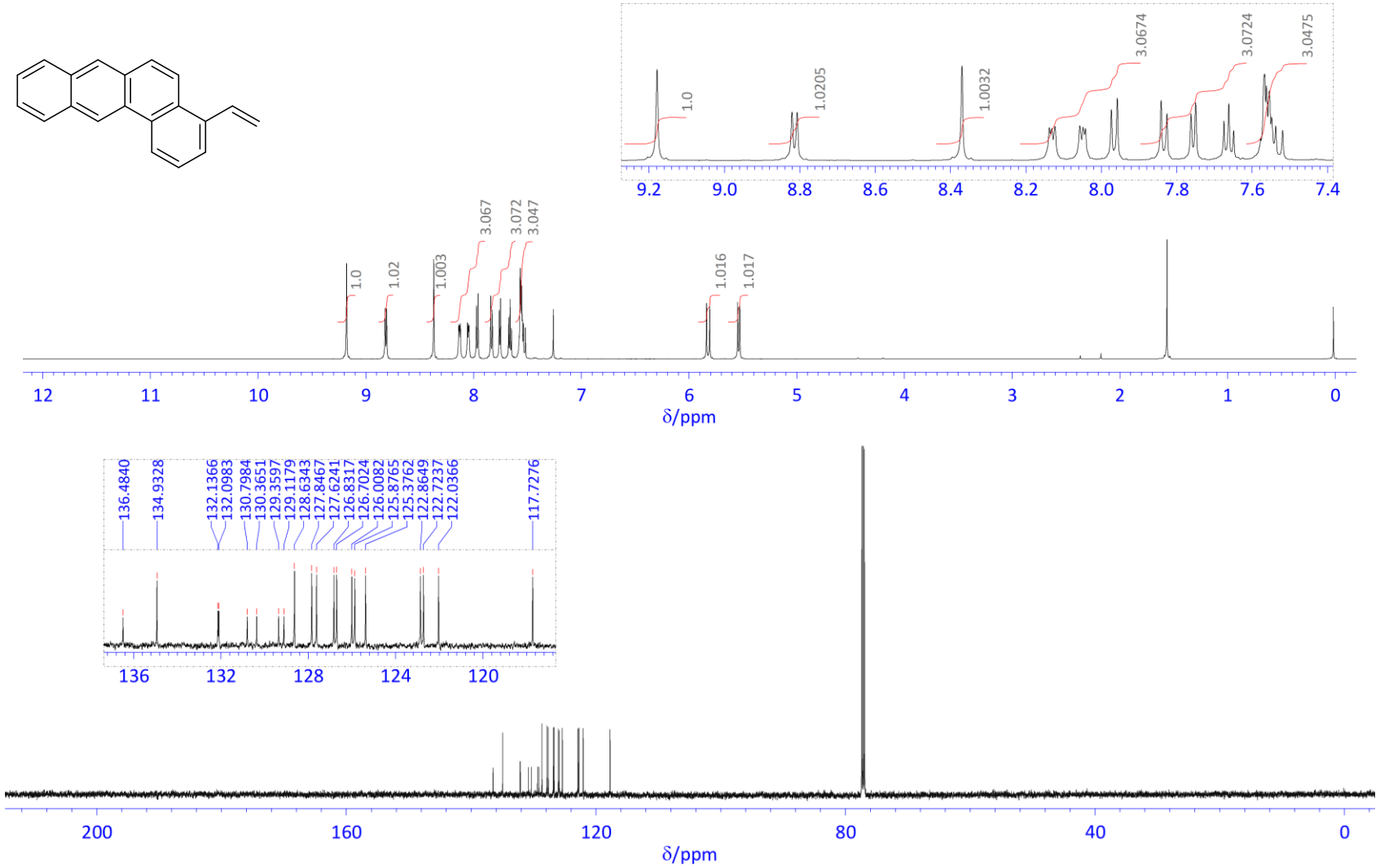

Figure S3. ^{1}H (600 MHz) and ^{13}C (151 MHz) NMR spectra of compound **4** ($CDCl_3$).

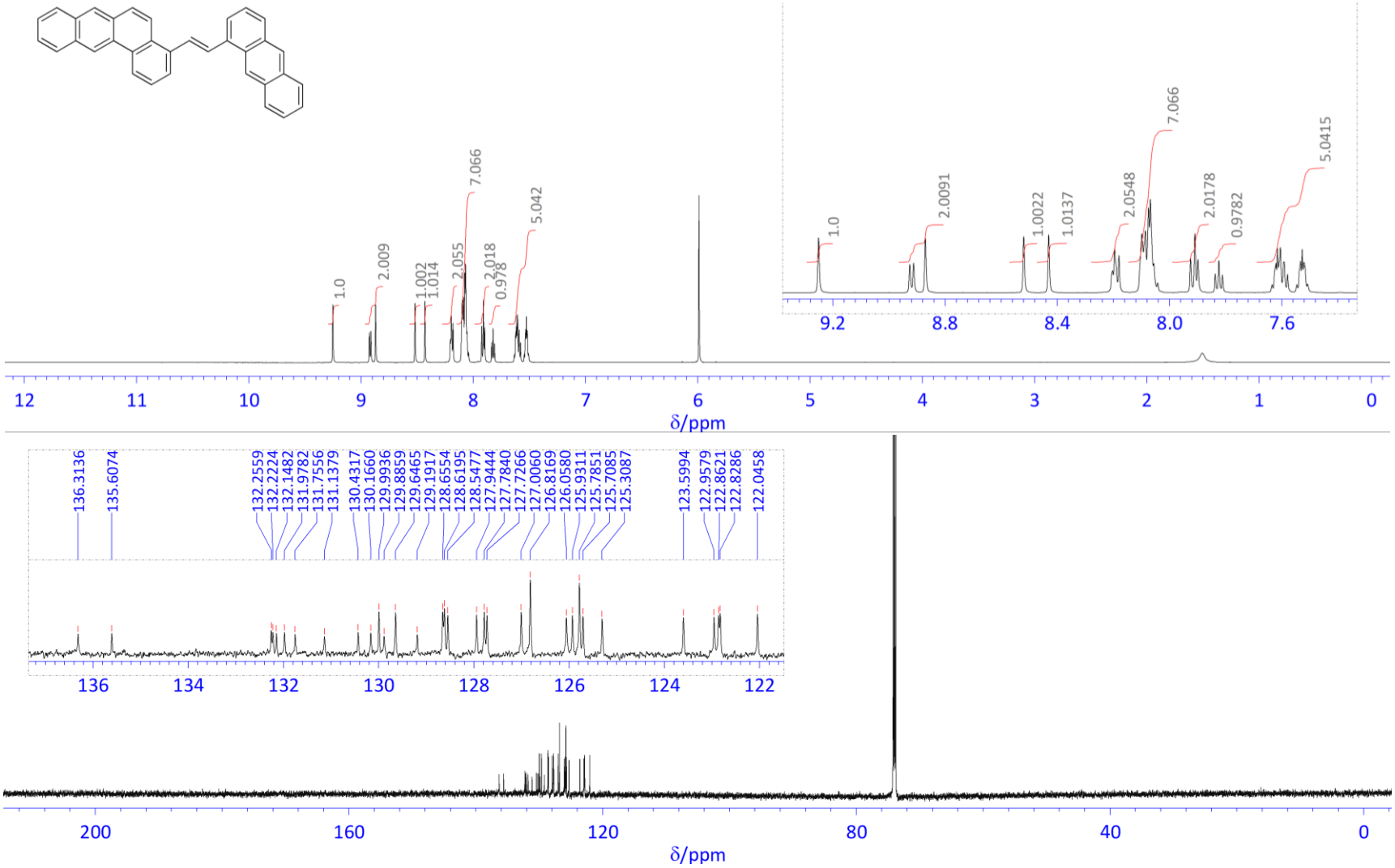

Figure S4. ^{1}H (600 MHz) and ^{13}C (151 MHz) NMR spectra of compound **5** (1,1,2,2-tetrachloroethane-d_2, at 80°C).

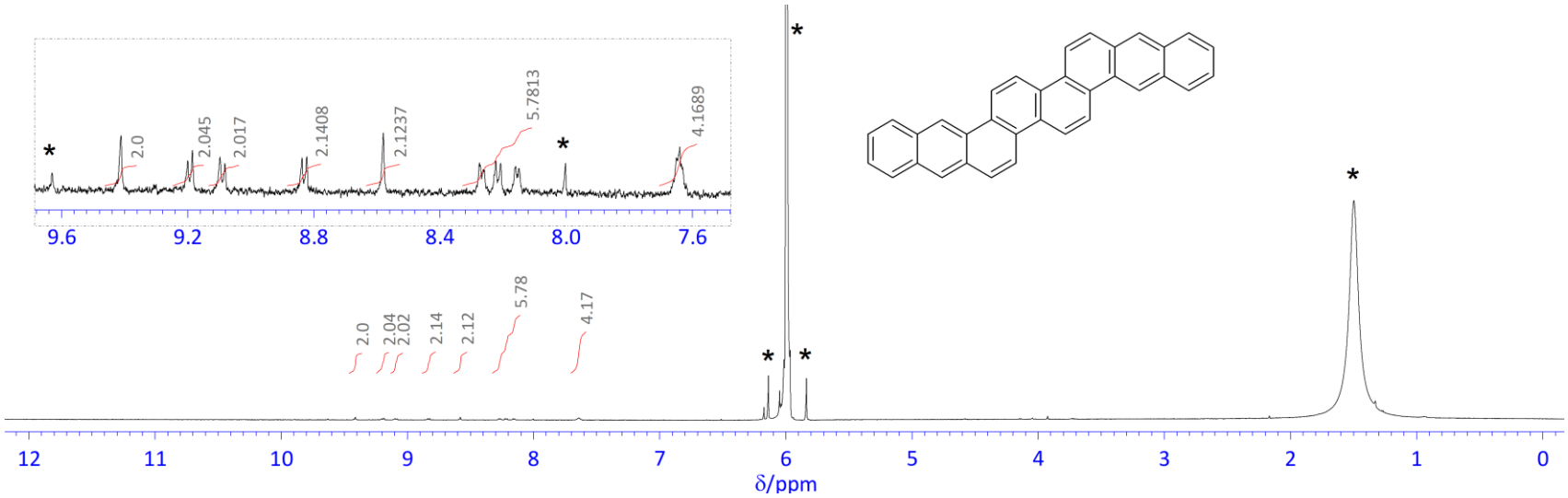

Figure S5. ^{1}H NMR spectrum of **DB6P** (600 MHz, 1,1,2,2-tetrachloroethane, at 95°C). Asterisked signals are due to the solvent, ^{13}C satellite, water, and impurity (inset).

3. X-ray diffraction (XRD) measurements and atomic force microscopy (AFM)

X-ray powder diffraction (XRPD) patterns of polycrystalline **DBnP** samples were measured at room temperature using synchrotron radiation at BL12B, SPring-8. The wavelength, λ, of x-ray beam was set to 0.5636 Å. X-ray diffraction patterns of **DBnP** thin films on SiO_2/Si substrate were measured at room temperature using an X-ray diffractometer (RIGAKU SMARTLAB-PRO) with CuKα radiation (λ = 1.5418 Å). The AFM image was measured with an AFM measurement system (SII Nano Technology SPA400). For the XRD and AFM measurements, a 60-nm thin-film of **DBnP** was formed on the SiO_2/Si substrate by thermal deposition under 10^{-7} Torr.

4. UV-Vis absorption and photoelectron yield measurements

Optical absorption was recorded with a UV-Vis absorption spectrometer (JASCO V-670 iRM EX). Photoelectron yield spectroscopy (PYS) was measured at room temperature under vacuum condition using a PYS spectrometer (Bunko-keiki BIP-KV200BS). 60-nm thick films of **DBnP**s formed on quartz and SiO_2/Si substrates were prepared for the measurements of the UV-Vis absorption and PYS spectra, respectively.

5. Synthesis of DBnP single crystals

Single crystals of **DBnP**s were prepared by the physical vapor transport method using synthesized powder samples of **DBnP**s. The polycrystalline samples (15-20 mg) of **DBnP**s were placed in a glass tube installed in the two-temperature-zone furnace, and for the preparation of single crystals the glass tube was heated to 240 and 400 ºC for **DB5P**, 280 and 430 ºC for **DB6P**, and 300 and 480 ºC for **DB7P**. During growth of single crystals, Ar gas was shed at 50 mL/min in the glass tube. The single crystals were collected in the lower temperature zone. The single crystals were transparent and plate-like (Figure S10). Their flat side was parallel to the *ab*-plane, and their thickness direction corresponds to the *c*-axis. 200-400 nm-thick crystals were used as active layers of single crystal FET devices.

6. Device fabrication of single-crystal FETs

Single crystals of **DBnP**s was placed on the SiO_2/Si substrate, in which SiO_2 (300 nm thick) was used as the gate dielectric. The surface of the SiO_2/Si substrate was coated with parylene to produce a hydrophobic surface. The thickness of the Au source/drain electrodes was 100 nm. 3 nm-thick 2,3,5,6-tetrafluoro-7,7,8,8-teracyano-quinodimethane (F_4TCNQ) was inserted into the space between the Au electrodes and the single crystal to reduce contact resistance. The Au source/drain electrodes and the F_4TCNQ were emplaced by thermal deposition at 10^{-7} Torr.

The FET characteristics were recorded using a semiconductor parametric analyser (Agilent B1500A) in an Ar-filled glove box. As seen in the device structures, the source electrode was grounded ($V_S = 0$). Negative voltage was applied to V_G and V_D in measurements of transfer and output curves. The measured transfer curves were analysed to determine the FET parameters (mobility (μ_{sat}), threshold voltage (V_{th}), on/off ratio and subthreshold swing (S)) using the general metal-oxide-semiconductor (MOS) transistor formula for a saturation regime:

$$I_D = \frac{\mu_{sat} W C_o}{2L}(V_G - V_{th})^2,$$

where I_D, V_G, V_{th}, W, L and C_o refer to drain current, gate voltage, threshold voltage, channel width, channel length and capacitance per area of gate dielectric, respectively. The channel width W and the length L for each device are listed in Tables S1-S4. The C_o values for SiO_2 (300 nm) and ZrO_2 (150 nm) covered with parylene were measured using a precision LCR meter (Agilent E4980A). The C_o of SiO_2 gate dielectrics for **DB5P**, **DB6P**, and **DB7P** single crystal FETs were 9.95 nF cm^{-2}, 9.31 nF cm^{-2} and 9.45 nF cm^{-2}, respectively, and that of ZrO_2 for **DB6P** single crystal FETs was 42.7 nF cm^{-2}, which was determined by extrapolation of the capacitance measured at 20 Hz - 1 MHz to 0 Hz. The condition for a saturation regime, $V_D > V_G - V_{th}$, was completely satisfied in the analysis of the transfer curve. The saturation was completely found in the output characteristics of all FET devices fabricated in this study.

7. Device fabrication of thin-film FETs

60 nm thick thin-films of **DBnP**s were formed for an active layer on solid gate dielectrics of 400 nm thick SiO_2 and 150 nm thick ZrO_2 by a thermal deposition of **DBnP**s under a vacuum of 10^{-7} Torr. The surface of the SiO_2 was coated with hexamethyldisilazane (HMDS) to produce a hydrophobic surface, while that of ZrO_2 was covered with 50 nm thick parylene. The shape of the thin film was determined by use of a metal mask. 3 nm thick F_4TCNQ was deposited on the **DBnP**s' thin films, and 50 nm thick source and drain electrodes were formed by the thermal deposition of Au on the F_4TCNQ. The device structure is top-contact bottom-gate type. The W and L for each device are listed in Tables S5-S8. The C_o value of SiO_2 for **DB5P**, **DB6P** and **DB7P** thin film FETs was 8.3 nF cm^{-2}, and that of ZrO_2 for **DB6P** thin film FETs was 42.7 nF cm^{-2}. The measured transfer curves were analysed to determine the FET parameters using the general MOS transistor formula for a saturation regime in the same matter as the analysis of single crystal FETs.

Results

1. X-ray diffraction patterns

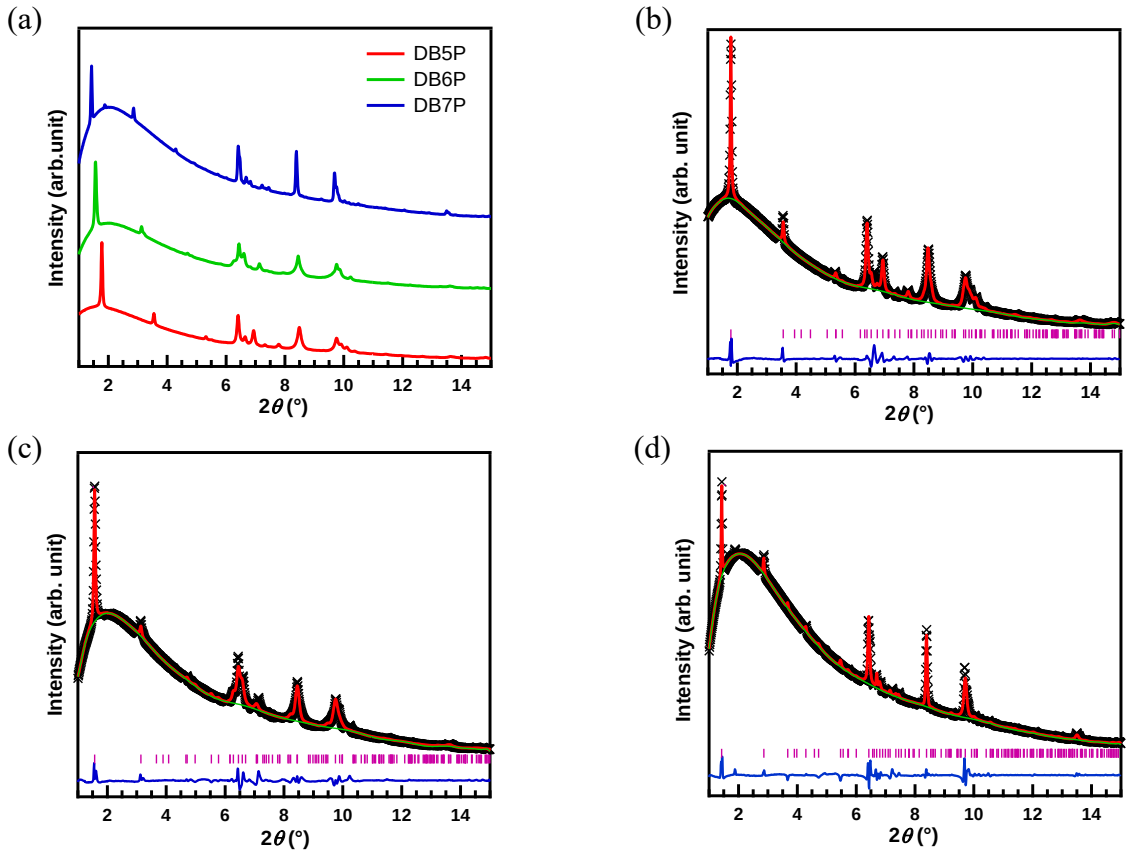

Figure S6. (a) Comparison of X-ray powder diffraction patterns of sublimed **DBnP** powders. X-ray diffraction patterns with the patterns calculated using Le Bail fitting of (b) **DB5P**, (c) **DB6P**, and (d) **DB7P**.

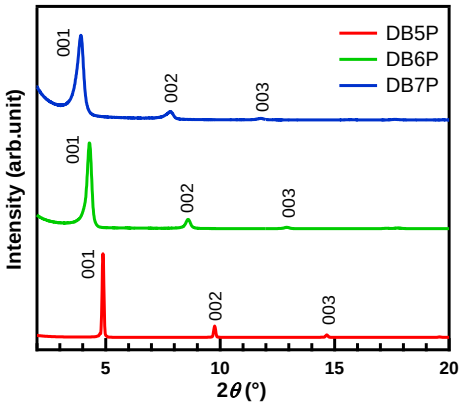

Figure S7. Comparison of X-ray diffraction patterns of **DBnP** thin films on SiO_2/Si substrates.

2. UV-Vis absorption and photoelectron yield spectra

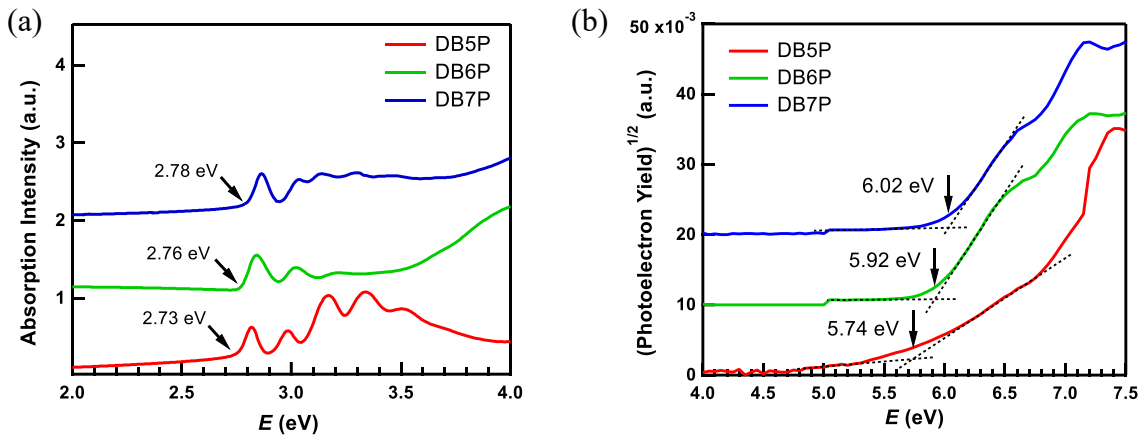

Figure S8. (a) UV-Vis absorption and (b) photoelectron yield spectra of **DBnP** thin films.

3. Surface morphology of DBnP thin films

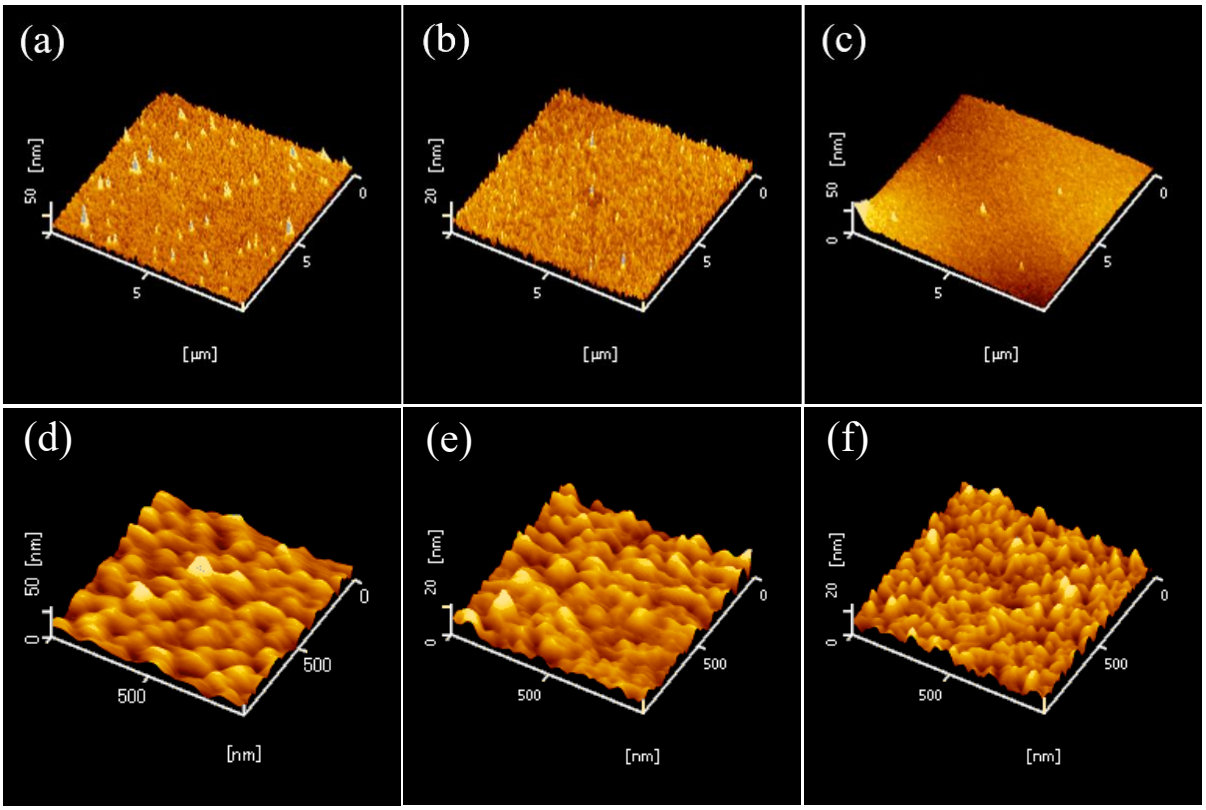

Figure S9. AFM images (10 μm × 10 μm scale) of (a) **DB5P**, (b) **DB6P**, and (c) **DB7P** thin films on SiO_2/Si substrates, respectively. (d), (e), and (f) are enlarged images (1 μm × 1 μm scale) of (a), (b), and (c), respectively.

4. Optical microscope images of DBnP single crystals

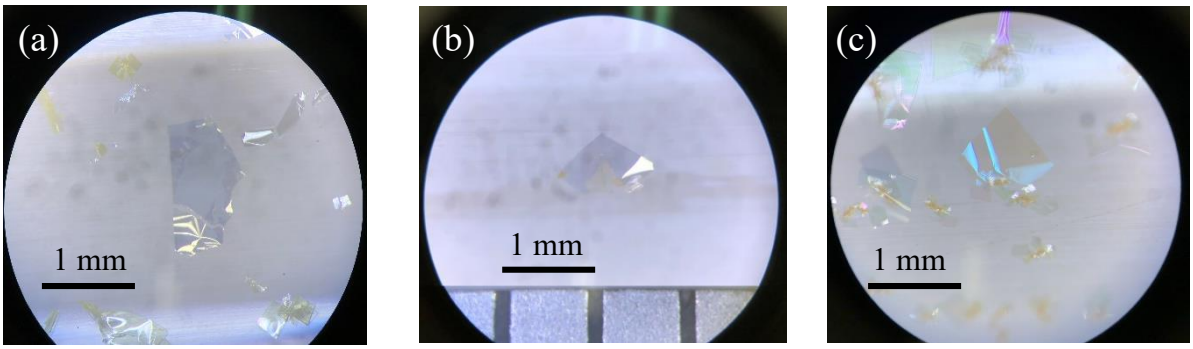

Figure S10. Optical microscope images of (a) **DB5P**, (b) **DB6P**, and (c) **DB7P** single crystals.

5. Typical FET performances of DBnP single crystal FETs

5-1. DBnP single crystal FETs with SiO_2 gate dielectric

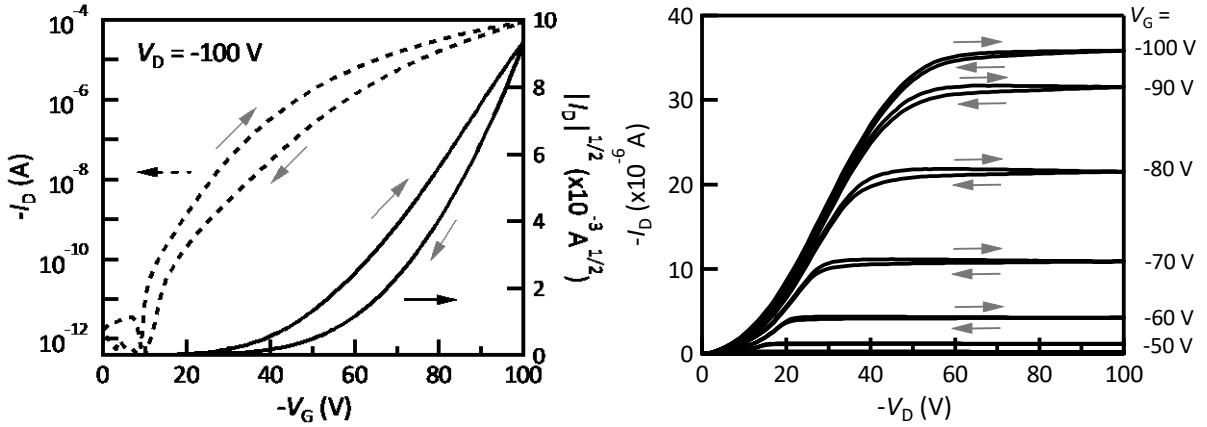

Figure S11. Transfer and output curves of **DB5P** single crystal FET with SiO_2 gate dielectric. This FET refers to device #4 in Table S1.

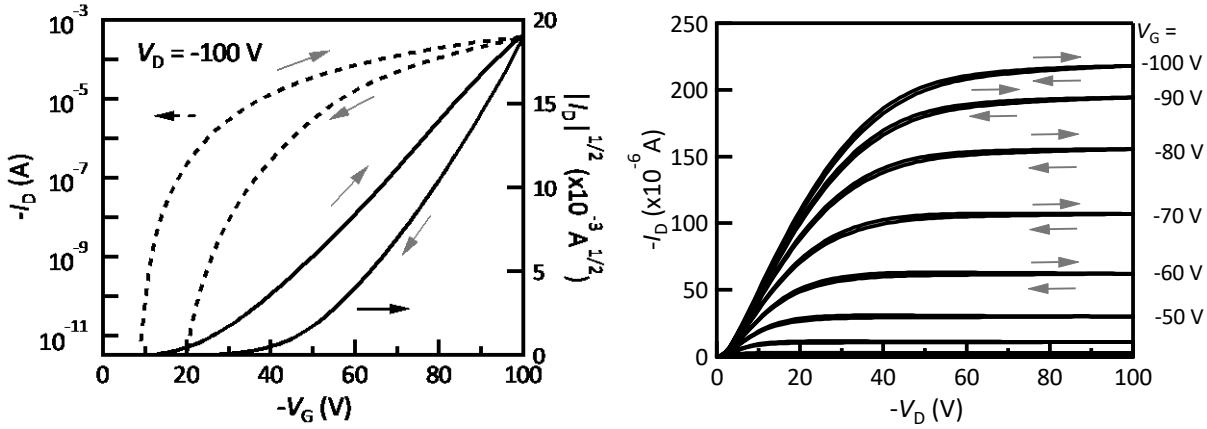

Figure S12. Transfer and output curves of **DB7P** single crystal FET with SiO_2 gate dielectric. This FET refers to device #2 in Table S3.

5-2. DBnP single crystal FETs with ZrO_2 gate dielectric

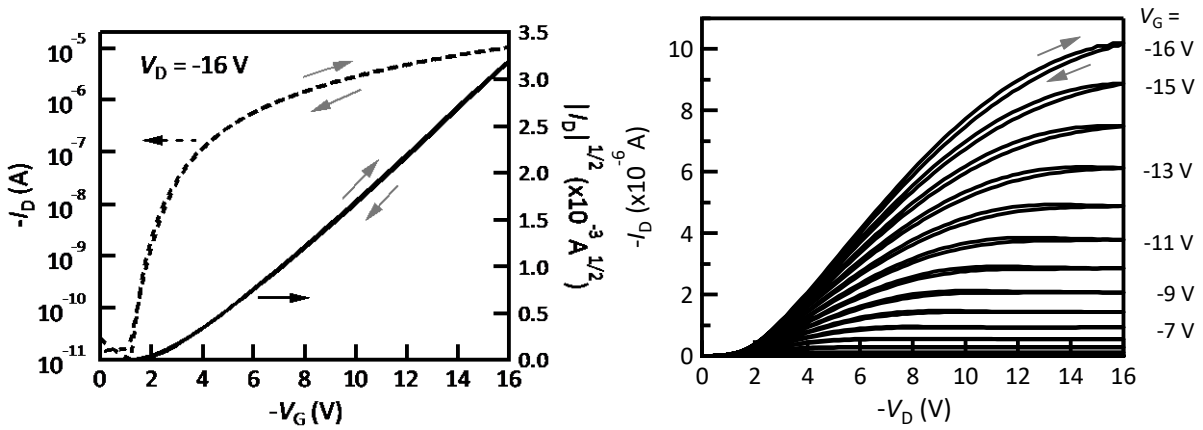

Figure S13. Transfer and output curves of **DB6P** single crystal FET with ZrO_2 gate dielectric. This FET refers to device #4 in Table S4.

6. Typical FET performances of DBnP thin film FETs

6-1. DBnP thin film FETs with SiO_2 gate dielectric

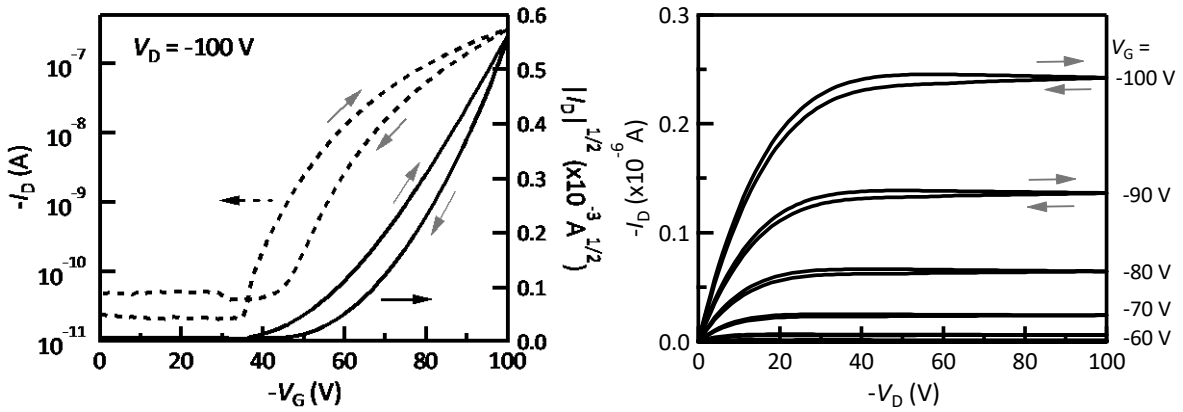

Figure S14. Transfer and output curves of **DB5P** thin film FET with SiO_2 gate dielectric. This FET refers to device #2 in Table S5.

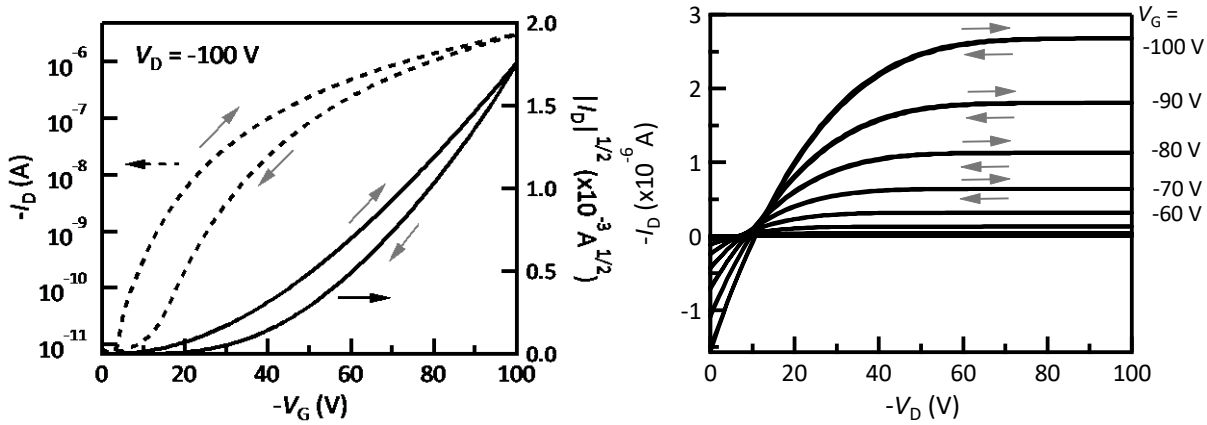

Figure S15. Transfer and output curves of **DB6P** thin film FET with SiO_2 gate dielectric. This FET refers to device #2 in Table S6.

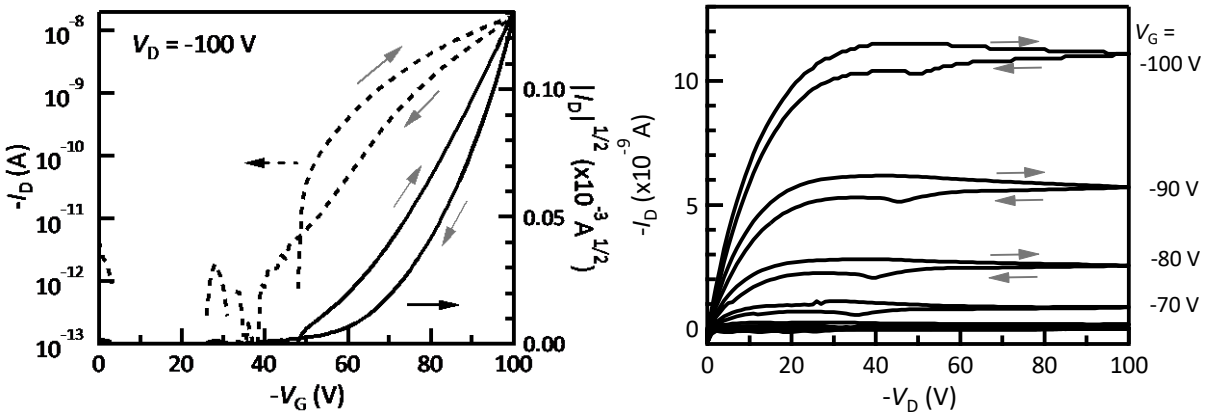

Figure S16. Transfer and output curves of **DB7P** thin film FET with SiO_2 gate dielectric. This FET refers to device #2 in Table S7.

6-2. DB6P thin film FETs with ZrO_2 gate dielectric

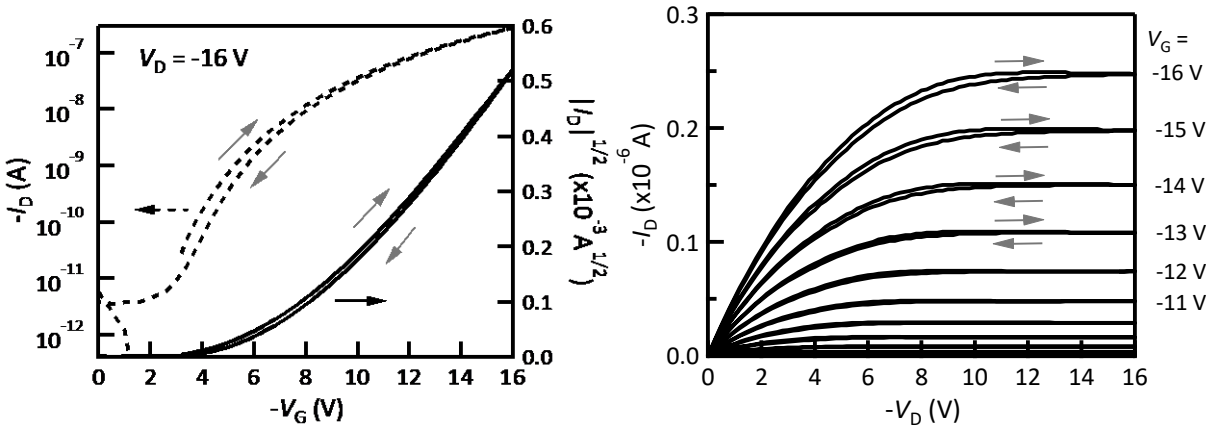

Figure S17. Transfer and output curves of **DB6P** thin film FET with ZrO_2 gate dielectric. This FET refers to device #4 in Table S8.

Tables

Table S1. FET parameters of **DB5P** single-crystal FETs with SiO_2 gate dielectric.

DB5P SC	μ_{sat} ($cm^2 V^{-1} s^{-1}$)	r_{sat}	μ_{eff} ($cm^2 V^{-1} s^{-1}$)	V_{th} (V)	on/off	S (V decade^{-1})	W/L (μm/μm)
#1	1.39	0.64	8.90×10^{-1}	19.4	3.25×10^{8}	1.71	300/250
#2	1.29	0.29	3.74×10^{-1}	45.8	9.16×10^{6}	3.48	410/200
#3	1.07	0.26	2.78×10^{-1}	49.1	1.54×10^{8}	1.34	250/150
#4*	3.21	0.25	8.03×10^{-1}	50.0	1.45×10^{8}	3.49	550/250
#5	1.55	0.22	3.41×10^{-1}	53.0	2.13×10^{7}	2.23	200/250
#6	1.41	0.21	2.96×10^{-1}	54.9	1.21×10^{7}	4.89	300/50
average	1.7(8)	0.3(2)	$5(3)\times10^{-1}$	50(10)	$1(1)\times10^{8}$	3(1)	

Table S2. FET parameters of **DB6P** single-crystal FETs with SiO_2 gate dielectric.

DB6P SC	μ_{sat} ($cm^2 V^{-1} s^{-1}$)	r_{sat}	μ_{eff} ($cm^2 V^{-1} s^{-1}$)	V_{th} (V)	on/off	S (V decade^{-1})	W/L (μm/μm)
#1	1.03	0.94	9.68×10^{-1}	2.84	1.84×10^{7}	1.48	315/50
#2	1.80	0.82	1.48	9.26	1.22×10^{8}	1.26	220/50
#3	2.19	0.76	1.66	12.6	3.36×10^{7}	1.88	580/450
#4	2.39	0.75	1.79	13.4	2.00×10^{7}	1.48	200/450
#5*	2.73	0.66	1.80	18.7	2.05×10^{7}	1.46	700/700
average	2.0(7)	0.8(1)	1.5(4)	11(6)	$4(4)\times10^{7}$	1.5(2)	

Table S3. FET parameters of **DB7P** single-crystal FETs with SiO_2 gate dielectric.

DB7P SC	μ_{sat} ($cm^2 V^{-1} s^{-1}$)	r_{sat}	μ_{eff} ($cm^2 V^{-1} s^{-1}$)	V_{th} (V)	on/off	S (V decade^{-1})	W/L (μm/μm)
#1	2.07	0.58	1.20	23.6	6.04×10^{7}	2.70	300/50
#2*	2.58	0.55	1.42	25.0	4.87×10^{7}	1.67	270/50
#3	1.35	0.54	7.29×10^{-1}	26.1	9.03×10^{6}	1.06	820/450
#4	1.76	0.53	9.33×10^{-1}	26.6	5.42×10^{6}	1.40	470/50
#5	1.70	0.34	5.78×10^{-1}	41.7	2.09×10^{8}	1.79	470/50
#6	1.48	0.28	4.14×10^{-1}	47.4	2.22×10^{7}	1.58	590/50
average	1.8(5)	0.5(1)	$9(8)\times10^{-1}$	30(10)	$6(8)\times10^{7}$	1.7(6)	

Table S4. FET parameters of **DB6P** single-crystal FETs with ZrO_2 gate dielectric.

DB7P SC	μ_{sat} ($cm^2 V^{-1} s^{-1}$)	r_{sat}	μ_{eff} ($cm^2 V^{-1} s^{-1}$)	V_{th} (V)	on/off	S (V decade^{-1})	W/L (μm/μm)
#1	2.06	0.75	1.55	2.16	7.49×10^6	0.30	175/50
#2	2.03	0.74	1.50	2.22	1.23×10^7	0.29	320/50
#3	2.06	0.73	1.50	2.33	1.48×10^7	0.28	345/50
#4*	2.54	0.63	1.60	3.32	1.01×10^6	0.39	525/450
average	2.2(3)	0.71(6)	1.54(5)	2.5(6)	$9(6)\times10^6$	0.32(5)	

Table S5. FET parameters of **DB5P** thin-film FETs with SiO_2 gate dielectric.

DB5P thin-film	μ_{sat} ($cm^2 V^{-1} s^{-1}$)	r_{sat}	μ_{eff} ($cm^2 V^{-1} s^{-1}$)	V_{th} (V)	on/off	S (V decade^{-1})	W/L (μm/μm)
#1	1.77×10^{-2}	0.19	3.36×10^{-3}	55.7	2.34×10^{4}	7.27	500/200
#2*	3.68×10^{-2}	0.18	6.62×10^{-3}	57.1	1.55×10^{4}	6.54	500/450
#3	2.92×10^{-2}	0.17	4.96×10^{-3}	58.2	8.52×10^{3}	7.67	500/450
#4	1.97×10^{-2}	0.17	3.35×10^{-3}	58.6	1.60×10^{4}	5.35	500/450
#5	1.32×10^{-2}	0.17	2.24×10^{-3}	58.7	1.48×10^{4}	7.09	500/250
#6	1.51×10^{-2}	0.12	1.81×10^{-3}	65.1	3.33×10^{4}	8.14	500/150
#7	1.71×10^{-2}	0.11	1.88×10^{-3}	66.7	9.41×10^{3}	7.71	500/300
#8	1.47×10^{-2}	0.11	1.62×10^{-3}	66.6	5.42×10^{3}	9.44	500/100
average	$2.0(8)\times10^{-2}$	0.15(3)	$3(2)\times10^{-3}$	61(5)	$1.6(9)\times10^{4}$	7(1)	

Table S6. FET parameters of **DB6P** thin-film FETs with SiO_2 gate dielectric.

DB6P thin-film	μ_{sat} ($cm^2 V^{-1} s^{-1}$)	r_{sat}	μ_{eff} ($cm^2 V^{-1} s^{-1}$)	V_{th} (V)	on/off	S (V decade^{-1})	W/L (μm/μm)
#1	5.70×10^{-2}	0.40	2.28×10^{-2}	36.6	3.16×10^{5}	2.62	1000/450
#2*	9.83×10^{-2}	0.38	3.74×10^{-2}	38.7	4.37×10^{5}	2.88	500/250
#3	7.82×10^{-2}	0.37	2.89×10^{-2}	39.7	4.61×10^{5}	4.54	500/50
#4	8.90×10^{-2}	0.35	3.12×10^{-2}	41.3	7.76×10^{5}	4.33	500/135
#5	6.74×10^{-2}	0.30	2.02×10^{-2}	45.7	3.86×10^{5}	3.46	1000/450
average	$8(2)\times10^{-2}$	0.36(4)	$2.8(7)\times10^{-2}$	40(3)	$5(2)\times10^{5}$	3.6(9)	

Table S7. FET parameters of **DB7P** thin-film FETs with SiO_2 gate dielectric.

DB7P thin-film	μ_{sat} ($cm^2 V^{-1} s^{-1}$)	r_{sat}	μ_{eff} ($cm^2 V^{-1} s^{-1}$)	V_{th} (V)	on/off	S (V decade^{-1})	W/L (μm/μm)
#1	8.11×10^{-4}	0.21	1.70×10^{-4}	54.1	8.71×10^{3}	2.96	1000/450
#2*	1.14×10^{-3}	0.16	1.82×10^{-4}	60.2	3.78×10^{3}	5.34	1000/450
#3	4.22×10^{-4}	0.14	5.91×10^{-5}	62.6	1.72×10^{3}	3.30	1000/450
average	$8(4)\times10^{-4}$	0.17(4)	$1.4(7)\times10^{-4}$	59(4)	$5(4)\times10^{3}$	4(1)	

Table S8. FET parameters of **DB6P** thin-film FETs with ZrO_2 gate dielectric.

DB6P thin-film	μ_{sat} ($cm^2 V^{-1} s^{-1}$)	r_{sat}	μ_{eff} ($cm^2 V^{-1} s^{-1}$)	V_{th} (V)	on/off	S (V decade^{-1})	W/L (μm/μm)
#1	7.74×10^{-2}	0.32	2.48×10^{-2}	6.98	7.28×10^{6}	0.43	500/50
#2	7.24×10^{-2}	0.31	2.24×10^{-2}	7.02	7.85×10^{5}	0.58	1000/450
#3	6.64×10^{-2}	0.31	2.06×10^{-2}	7.03	1.93×10^{4}	1.52	1000/450
#4*	8.10×10^{-2}	0.30	2.43×10^{-2}	7.15	9.98×10^{3}	0.54	500/250
#5	7.89×10^{-2}	0.20	1.58×10^{-2}	8.91	1.21×10^{5}	0.49	500/135
average	$7.5(6)\times10^{-2}$	0.29(5)	$2.2(4)\times10^{-2}$	7.4(8)	$2(3)\times10^{6}$	0.7(5)	

Additional References

1. Y. Takeuchi, S. Akiyama and M. Nakagawa, *Bull. Chem. Soc. Jpn.*, 1972, **45**, 3183.
2. B. P. Cho and R. G. Harvey, *J. Org. Chem*., 1987, **52**, 5668.